IOPscience iopscience.iop.org

Home Search Collections Journals About Contact us My IOPscience

Critical behaviour of random surfaces on the cubic lattice

This article has been downloaded from IOPscience. Please scroll down to see the full text article.

1986 J. Phys. A: Math. Gen. 19 3375

(http://iopscience.iop.org/0305-4470/19/16/033)

View the table of contents for this issue, or go to the journal homepage for more

Download details:
IP Address: 129.252.86.83
The article was downloaded on 31/05/2010 at 10:52

Please note that terms and conditions apply.

J. Phys. A: Math. Gen. 19 (1986) 3375-3393. Printed in Great Britain

Critical behaviour of random surfaces on the cubic lattice

M Karowski†

Institut für Theorie der Elementarteilchen, Fachbereich Physik, Freie Universität Berlin, Arnimallee 14, D-1000 Berlin 33, West Germany

Received 22 November 1985

Abstract. The phase diagram and the critical behaviour of an (intersecting) random surface gas model in three dimensions is studied by means of Monte Carlo simulations. The critical exponents α, β, γ and δ are evaluated in the 'critical window' between the finite-size rounding and the correction-to-scaling regime. Within error bars, Ising exponents for the self-avoiding case (and along critical lines) and mean-field behaviour at tricritical points are obtained. For the self-avoiding planar surface model the Hausdorff dimension is calculated ($d_H = 2.30 \pm 0.05$).

1. Introduction

Recently [1] we analysed the phase structure of self-avoiding random surface gas models. In the present paper related models of random surfaces on cubic lattices in three dimensions are investigated. The phase structure is determined and the critical exponents and the corresponding amplitudes are calculated. Random surfaces are a useful concept in different regions of physics. Quantum field theories can be formulated in terms of random walks (polymers) [2]. Analogously, it is widely believed (cf [3] and references therein) that non-Abelian gauge theories are in some way related to random surfaces in $d = 4$ dimensions. An investigation of the critical behaviour should lead to a better understanding of gauge and dual string theories [4] in their continuum limits.

Furthermore, self-avoiding random surfaces in three dimensions might [5] be useful for the understanding of microemulsions whose stability relies on a balance of entropy and energy of the interfaces (see [6] and references therein). They can also be expected to describe properties of flexible two-dimensional sheet polymers [7]. The self-avoiding random surface model is a natural generalisation of the solid-on-solid model [8] which is useful for describing the roughening of crystal surfaces and interfaces. For previous Monte Carlo simulations of random surfaces see also [9, 10].

In reference [1] we investigated by means of Monte Carlo simulations a self-avoiding random surface gas model defined by the partition function

$$Z = \sum_{c \in \mathcal{C}_{SAS}} \exp[-\beta_s s(c)] \tag{1}$$

where the sum extends over all configurations of closed self-avoiding surfaces on a

† Present address: Physique Théorique et Hautes Energies, Université Paris VI, Tour 16-le étage, 4 place Jussieu, F-75230 Paris, Cedex 05, France.

0305-4470/86/163375+19$02.50 © 1986 The Institute of Physics

domain L^3 of the cubic lattice. A configuration $c \in \mathscr{C}_{\mathrm{SAS}}$ comprised a (possibly disconnected) collection of plaquettes in the lattice such that each link in c is contained in two plaquettes. The energy of c is taken to be proportional to the total surface $s(c)$ = number of plaquettes in c and $\beta_s = \varepsilon_s / kT$ with ε_s = energy of one plaquette. In addition we considered in [1] generalisations on this model introducing curvature energies or chemical potentials for topological quantities like the Euler characteristic and analysed the phase structure. Our previous [11] investigation of the two-dimensional self-avoiding loop gas model by means of Monte Carlo simulations we recently continued with a detailed study of the critical behaviour [12]. The critical exponents α, β, γ and δ were evaluated in the 'critical window' between the finite-size rounding and the non-critical (correction-to-scaling) regime. Since the critical temperature is known rather accurately (to 0.1%) [13] and since we could use large lattices (up to $L = 80$) with reasonable computer times we were able to calculate the exponents with small error bars and obtained Ising behaviour.

In the present paper this method is applied to the three-dimensional self-avoiding surface gas model. However, the situation in this case is worse for two reasons: (i) the critical temperature is not known with comparable accuracy (to 2%) [1] and (ii) reasonable computer times restrict the lattice size to $L \leqslant 26$. Therefore the critical window is rather narrow. The order parameter (see § 2) which indicates the phase transition has a symmetry which suggests Ising-like critical behaviour for the self-avoiding surface gas model. Therefore it is useful to extend the model to a class which also contains, as a special case, the Ising model. This is the intersecting surface gas model discussed by Sterling and Greensite [9]. It is defined by the partition function

$$Z(\beta_s, \beta_l) = \sum_{c \in \mathscr{C}} \exp[-\beta_s s(c) - \beta_l l(c)]. \tag{2}$$

The sum runs over all closed surfaces $c \in \mathscr{C}$ (including intersecting ones). The intersection energy is proportional to the total intersection length $l(c)$, i.e. the number of the links contained in four plaquettes on the surface c and $\beta_l = \varepsilon_l / kT$ with ε_l = energy per link. For vanishing intersection energy $\beta_l = 0$ the model is equivalent to the Ising model on the dual lattice (a surface c can be identified with the Peierls interfaces of an Ising configuration) and to the $Z(2)$ gauge model [21] (a surface c can be identified with a high-temperature expansion graph of the $Z(2)$ gauge model). In the limit of extremely strong repulsive interactions along the intersections $\beta_l \to \infty$ we obtain the self-avoiding surface gas model defined by (1). The phase structure of model (2) was analysed by Monte Carlo simulations in reference [9]. We will see in § 3 that the phase diagram is more complicated. In the β_s, β_l plane there are lines of second- and first-order phase transitions, tricritical points and a point where five phases coexist.

A configuration of model (2) can be generated on a computer iteratively as follows. Starting from an old configuration one gets a new one by a local change in a unit cube. A local change means the replacement of empty plaquettes by occupied ones and vice versa (i.e. the 'change a cube' operation of reference [9]). By a Monte Carlo simulation one generates samples of equilibrium ensembles of configurations c_i. In the heat bath updating procedure one sequentially sweeps all L^3 unit cubes and accepts the new configuration with probability

$$w_{\mathrm{new}} / (w_{\mathrm{old}} + w_{\mathrm{new}}) \tag{3}$$

where the w are the Boltzmann factors

$$w = \exp(-\mathrm{energy}/kT). \tag{4}$$

The thermal average of a variable A is then approximated by

$$\langle A\rangle \approx \frac{1}{N}\sum_{i=1}^{N} A(c_i). \tag{5}$$

By this Monte Carlo method the energy, specific heat, order parameter and susceptibility near to some points along the critical line and tricritical points are computed. Consistency with Ising behaviour along the critical lines and mean-field behaviour at the tricritical points is obtained.

The paper is organised as follows. In § 2 symmetry properties of the intersecting surface gas model are derived and order parameters are defined. Section 3 presents a discussion of the phase diagram. In §§ 4 and 5 the critical behaviour of the self-avoiding and the intersecting surface gas model, respectively, is analysed by means of Monte Carlo simulations. In § 6 the 'Hausdorff dimension' d_H of a self-avoiding planar surface model is determined. Section 7 contains concluding remarks as well as a table of the results for the critical and tricritical exponents α, β, γ, δ, α_t, β_t, γ_t, δ_t and the amplitudes $A^{\pm}$, B, $C^{\pm}$, D, A_t^-, B_t, C_t^- and D_t.

2. The intersecting surface gas model

In this section we derive symmetry properties and define order parameters of the intersecting surface gas model defined by the partition function (2). Any configuration $c \in \mathscr{C}$ of closed surfaces contributing in equation (2) is given by a collection of numbers $s(x, i, j)$ defined on all plaquettes (i, j), $1 \leq i < j \leq 3$, at all lattice points $x \in L^3$. We set $s(x, i, j) = 1$ or 0, if the plaquette belongs to the surfaces of the configuration c, or not, respectively. The total surface is then

$$s(c) = \sum_{x, i<j} s(x, i, j). \tag{6}$$

Analogously, we define on all links $i = 1, 2, 3$ at all lattice points $x \in L^3$ the function $l(x, i) = 1$ or 0 if the link belongs to the intersection lines of the surfaces of a configuration c, or not, respectively, such that the total intersection length is

$$l(c) = \sum_{x,i} l(x, i). \tag{7}$$

The set of closed surfaces $\mathscr{C}$ is obviously invariant under the transformation $c \to c'$ defined by

$$s(x, i, j) \to s'(x, i, j) = 1 - s(x, i, j) \tag{8}$$

with the trivial transformation law for the total surface

$$s(c) \to s(c') = 3L^3 - s(c). \tag{9}$$

For the intersection length the following transformation law holds:

$$l(c) \to l(c') = l(c) - 2s(c) + 3L^3. \tag{10}$$

This is not so obvious but can be verified by analysing the neighbourhood of any link under the transformation $c \to c'$ (see below). Hence we have a symmetry property of the intersecting surface gas model which can be expressed by

$$Z(\beta_s, \beta_l) = \exp[-3L^3(\beta_s + \beta_l)]Z(-\beta_s - 2\beta_l, \beta_l). \tag{11}$$

For vanishing intersection energy $\beta_I = 0$ this is the well known ferro-antiferromagnetic symmetry of the Ising model.

Another formulation of the intersecting surface gas model is analogous to the eight-vertex formulation of the loop gas model in two dimensions (cf [13]):

$$Z = \sum_{\{\omega\}} \prod_{x \in L^3} \prod_{i=1}^{3} \omega(x, i) \tag{12}$$

where the sum extends over vertex configurations at the links of the lattice: $\omega(x, i) = \omega_1, \ldots, \omega_8$ with $\omega_1 = \exp(\beta_s/2)$, $\omega_2 = \exp(-\beta_s/2 - \beta_I)$, $\omega_3 = \cdots = \omega_8 = 1$ with the standard assignment given in figure 1. The transformation $c \to c'$ defined by (8) means $\omega_1 \leftrightarrow \omega_2$, $\omega_3 \leftrightarrow \omega_4$, $\omega_5 \leftrightarrow \omega_6$, $\omega_7 \leftrightarrow \omega_8$. In this formulation the proof of (10) is simpler.

Motivated by the Ising spin $\sigma(x)$ it is obvious to define the local order parameter $\sigma(x)$ and a staggered one $\sigma'(x)$ for the general intersecting surface gas model (2). A closed surface divides the lattice L^3 into two parts, an inside and an outside region. Hence there exists a unique function $\sigma(x)$ on the lattice points $x \in L^3$ for any configuration (with the arbitrary normalisation $\sigma(0) = 1$) such that

$$\sigma(x) = \begin{cases} 1 & \text{if } x \text{ is outside } c \\ -1 & \text{if } x \text{ is inside } c. \end{cases} \tag{13}$$

In order to preserve the symmetry

$$\sigma(x) \to -\sigma(x) \tag{14}$$

we replace in the following the set of configurations $\mathscr{C}$ in (2) by $\mathscr{C}_+ \cup \mathscr{C}_-$ where $\mathscr{C}_\pm = \mathscr{C}$ and $c \in \mathscr{C}_\pm \Leftrightarrow \sigma(0) = \pm 1$. There exists also a spin formulation of the intersecting surface gas model (2)

$$Z = \sum_{\{\sigma\}} \exp\left(J_1 \sum_{\text{NN}} \sigma\sigma + J_2 \sum_{\text{NNN}} \sigma\sigma + J_3 \sum_{\text{plaq}} \sigma\sigma\sigma\sigma \right) \tag{15}$$

with nearest (NN), next-nearest (NNN) and around a plaquette (plaq) interactions $J_1 = \beta_s/2 + \beta_I/2$ and $J_2 = J_3 = -\beta_I/8$.

Under the symmetry transformation (8) the spin $\sigma(x)$ goes over into the staggered one

$$\sigma(x) \to \sigma'(x) = (-1)^{x_1 + x_2 + x_3} \sigma(x). \tag{16}$$

Let $\sigma(\sigma')$ be the site-averaged (staggered) spin

$$\sigma^{(\prime)} = \sum_{x \in L^3} \sigma^{(\prime)}(x)/L^3 \tag{17}$$

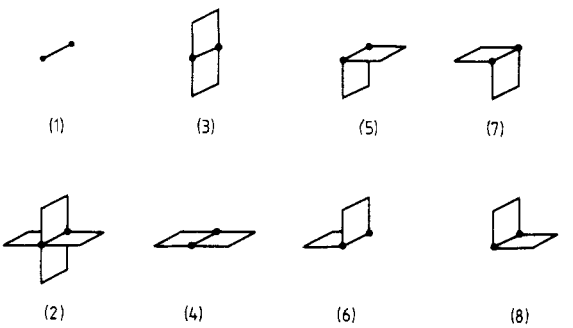

Figure 1. Vertex assignment at a link on the cubic lattice.

then the (staggered) 'magnetic' order parameter is defined by the statistical average

$$m^{(\prime)} = \langle \sigma^{(\prime)} \rangle. \tag{18}$$

The symmetry of the model which corresponds to the order parameter $m^{(\prime)}$ is a $Z(2)$ one (cf (14)). Therefore, if a second-order phase transition exists from the symmetric ($m^{(\prime)} = 0$) high-temperature phase to a symmetry breaking ($m^{(\prime)} \neq 0$) low temperature phase, the transition should be Ising-like. This will be verified in §§ 4 and 5 by means of Monte Carlo simulations. An external (staggered) 'magnetic' field $h^{(\prime)}$ corresponding to the order parameter $m^{(\prime)}$ will be introduced by

$$Z(\beta_s, \beta_l, h, h') = \sum_{c \in \mathscr{C}} \exp[-\beta_s s(c) - \beta_l l(c) + h\sigma + h'\sigma']. \tag{19}$$

Along the line $\beta_l = -\beta_s$ there exists in addition an 'electric' order parameter, 'polarisation',

$$p = \left\langle \sum_{\text{plaq}} p(x, i, j)/L^3 \right\rangle \tag{20}$$

with the local field defined on the plaquettes

$$p(x, i, j) = s(x, i, j) - \tfrac{1}{2}. \tag{21}$$

The denotation 'electric' is motivated by the vertex formulation (12) of the model (cf [14]). By (6) the 'polarisation' is related to the total surface average

$$p = \langle s \rangle / L^3 - \tfrac{3}{2}. \tag{22}$$

Therefore an external 'electric' field can be identified with $-\beta_s$. The symmetry group along $\beta_l = -\beta_s$ is $Z(2) \times Z(2)$

$$\begin{aligned} &p(x, i, j) \to -p(x, i, j) \\ &\sigma(x) \to -\sigma(x). \end{aligned} \tag{23}$$

Hence a critical point should not be Ising-like. As we will see in § 3 there exists a first-order transition from a symmetric ($p = 0$, $m = m' = 0$) to a symmetry breaking phase ($p \neq 0$, $m \neq 0$ or $m' \neq 0$).

3. The phase diagram of the model

The phase diagram of the intersecting surface gas model defined by (2) was already roughly discussed in reference [9] by means of Monte Carlo simulations, cf figure 2. The Monte Carlo results presented in this paper support this picture only up to some modifications discussed below. A disordered phase for small $\beta_s - \beta_l$ with $m = m' = 0$ is separated by a second-order phase transition line from an ordered ferro- (antiferro)magnetic one for large (small) $\beta_s + \beta_l$ with $m \neq 0$, $m' = 0$ ($m = 0$, $m' \neq 0$). The critical Ising point is at $(\beta_s, \beta_l)^c = (0.443, 0)$ and for the self-avoiding random surface gas model $\beta_l \to \infty$ our Monte Carlo data (see also § 4) imply

$$\beta_s^c = 0.353 \pm 0.001. \tag{24}$$

For small β_l the line $\beta_l = -\beta_s$ of first-order phase transitions separates the ordered phases. However, the juncture region of all phases near $\beta_s = -\beta_l = 0.609$ is more

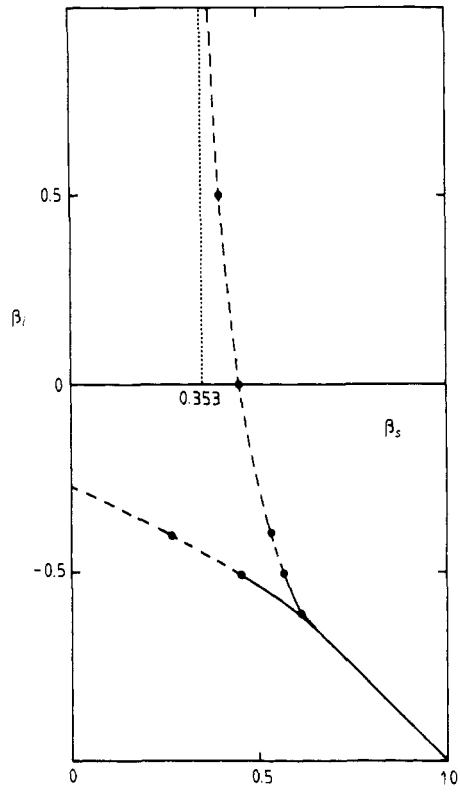

Figure 2. Phase diagram of the intersecting random surface gas model in the β_s, β_l plane showing first- (full curve) and second- (broken curve) order phase transition lines; (●) are Monte Carlo data. The line of symmetry is given by $\beta_s + \beta_l = 0$.

complicated than supposed in reference [9]. The intersecting surface model in three dimensions is analogous to the intersecting loop model in two dimensions

$$Z = \sum \exp[-\beta_l l(c) - \beta_i i(c)]$$

where $l(c)$ is the total loop length and $i(c)$ is the number of intersecting points. The phase diagram of this model which is equivalent to an asymmetric eight-vertex model (cf equation (12)) was analysed in reference [13] and is qualitatively identical to that shown in figure 2 (replacing β_s by $2\beta_l$ and β_l by β_i). Along the line $2\beta_l + \beta_i = 0$ the model is a solvable Baxter model with a non-Ising-like (cf the remarks after equation (23)) second-order phase transition at $\beta_l = -\beta_i/2 = \ln 3$. This point is a juncture of the two lines of second- and the one line of first-order phase transitions in the β_l, β_i plane. In the three-dimensional parameter space β_l, β_i, $h = h'$ the point is a tetracritical point where four critical lines meet tangentially a first-order transition line, a phase structure similar to that of the two-dimensional Potts model [15]. However, in three dimensions the zero-field Potts model is generally believed to show a first-order transition and the phase diagram is more complicated. Our Monte Carlo simulations show similar behaviour for the intersecting surface gas model. The juncture region mentioned above is shown in figure 3 in a $\beta_s + \beta_l$, β_l plane where the symmetry (8) is

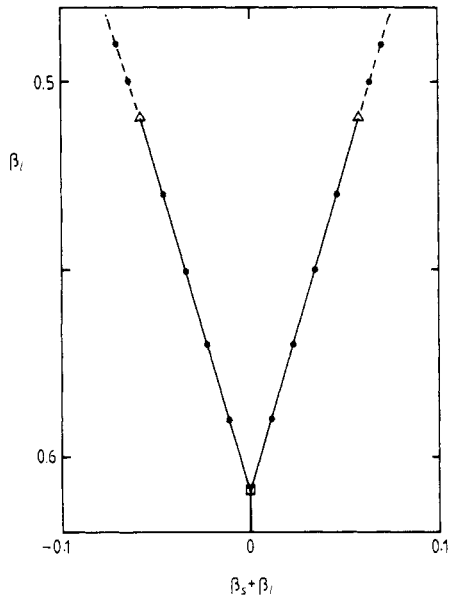

Figure 3. A cutting out of figure 2 (in the $\beta_s+\beta_l$, β_l plane) in the neighbourhood of the tricritical points (△) and the point (□) where the disordered phase coexists with four ordered ones; (●) are Monte Carlo data.

more conspicuous. Along the line $\beta_s+\beta_l=0$ we observe a first-order phase transition at

$$\beta_s^{(5)}=-\beta_l^{(5)}=0.609\pm0.001. \tag{25}$$

At this point five phases coexist: a disordered one with $m=m'=0$ and four ordered ones with $m\gtrless 0$, $m'=0$ and $m=0$, $m'\gtrless 0$. Along the first-order transition line $\beta_s+\beta_l=0$, $\beta_l<\beta_l^{(5)}$ the four ordered phases coexist. At the point $(\beta_s, \beta_l)^{(5)}$ another first-order

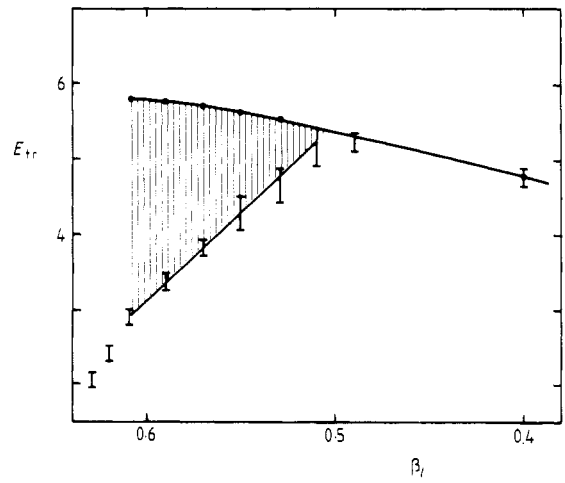

Figure 4. The energy against β_l diagram corresponding to figure 3 showing the transition energies and the energy jump at the first-order transition line.

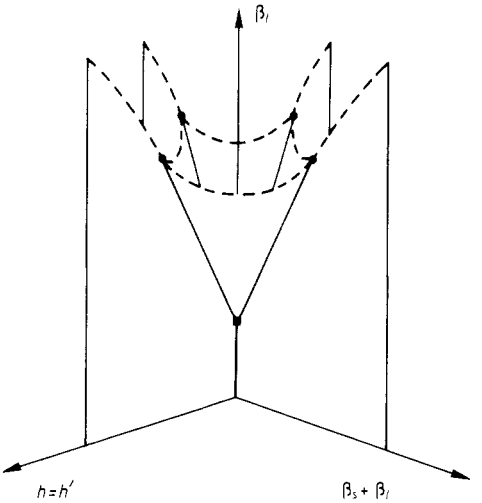

Figure 5. Schematic phase diagram of the intersecting random surface model in the $\beta_s+\beta_l$, β_l, $h=h'$ space showing eight coexistence planes, four tricritical points and critical lines (broken curves).

transition line starts where the disordered phase coexists with two ordered ones $m \gtrless 0$, $m'=0$ and pass over at a tricritical point $(\beta_s, \beta_l)^t$ to the critical line discussed above. By means of 'mixed start' Monte Carlo simulations on a $22\times22\times44$ lattice the transition points, the transition energies and the tricritical point were determined:

$$(\beta_s, \beta_l)^t = (0.568, 0.510) \pm \left\{\begin{matrix} 0.1 \text{ parallel} \\ 0.001 \text{ perpendicular} \end{matrix}\right\} \text{ to the transition line.} \tag{26}$$

Because of the symmetry (8) the analogue holds true for $m \leftrightarrow m'$ and $\beta_s+\beta_l \leftrightarrow -\beta_s-\beta_l$.

The energy/$kT=\langle\beta_s s+\beta_l l\rangle$ against β_l diagram in figure 4 shows the transition energies and the jump along the first-order transition line. The complete phase diagram in the three-dimensional parameter space $\beta_s+\beta_l$, β_l, $h=h'$ is depicted qualitatively in figure 5.

4. Critical behaviour of the self-avoiding surface gas model

In this section the critical exponents and amplitudes of the self-avoiding surface gas model in three dimensions are calculated by a method applied recently [12] to the analogous loop model in two dimensions. The order parameter, magnetisation, is defined by (18), and (19) yields

$$m=\langle\sigma\rangle=\frac{\partial}{\partial h}\ln Z(\beta_s, \infty, h, 0)|_{h=0}. \tag{27}$$

It should vanish above a critical temperature T_c and should show power behaviour below (near) T_c defining the critical exponent β and the amplitude B:

$$m \approx B|\varepsilon|^{\beta} \qquad T \uparrow T_c \tag{28}$$

with

$$\varepsilon=(T-T_c)/T. \tag{29}$$

The Monte Carlo data confirm this behaviour, cf figure 6 where the order parameter m is plotted against the temperature T (in units of ε_s/k). Any value is calculated (in a thermal loop) as an average over 500 configurations each obtained after five complete sweeps through the 26^3 lattice. Log-log plots of the data for lattices of size $L=10$, 20, 26 are given in figure 7 where $\ln(m)$ is plotted against $\ln|\varepsilon|$. The critical behaviour (28) should show up in a linear behaviour of the data in the 'critical window'. This region is bounded away from T_c by corrections to scaling (which depend on the physical quantity to be considered) and near to T_c by finite-size rounding effects (which depend on the lattice size L, i.e. on the computer time). This size dependence shows up in figure 7. In the previous investigation of the loop gas model [12] we profited from an accurate value of the critical temperature obtained in reference [13] with a finite-size transfer matrix method. Unfortunately, for the self-avoiding surface gas model there exists only a rather uncertain Monte Carlo value $\beta_c=0.36\pm0.01$ [1]. However, the 'critical window' method also yields a procedure to get a rather accurate value of the critical temperature. One chooses that value for T_c in equation (29) which implies the 'largest critical window', i.e. the longest linear behaviour in the plots of figure 7 for all lattice sizes L. With this method we obtain for the critical temperature of the self-avoiding surface gas model $T_c=\varepsilon_s/k\beta_s^c$ with

$$\beta_s^c=0.353\pm0.001. \tag{30}$$

The linear fit in figure 8 implies for the lattice size $L=26$ effective values for the exponent and the amplitude

$$\beta_{26}=0.29\pm0.01 \tag{31}$$

$$B_{26}=1.4\pm0.1. \tag{32}$$

A finite-size extrapolation to $L=\infty$ gives

$$\beta=0.32\pm0.01$$

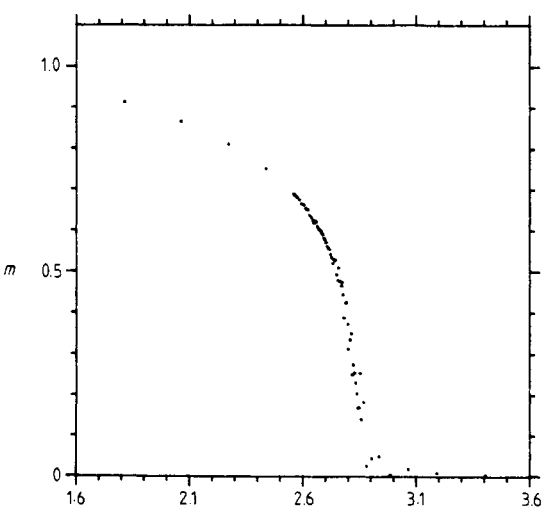

Figure 6. Monte Carlo results for the self-avoiding random surface gas model. The order parameter $|m|$ calculated on a cubic lattice of size $L=26$ with periodic boundary conditions is plotted against the temperature T in units of ε_s/k. The data indicate a second-order phase transition at $T_c=2.83$.

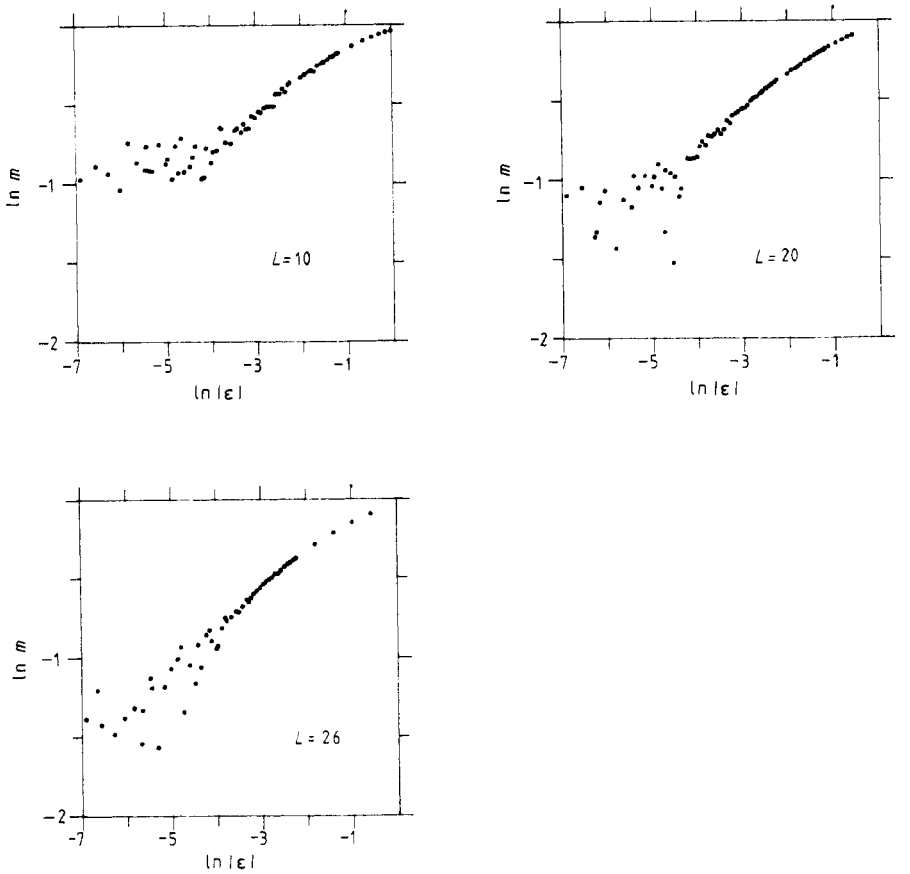

Figure 7. Log-log plots of the order parameter $\ln|m|$ against $\ln|\varepsilon|$ ($\varepsilon = (T - T_c)/T$) for $L = 10$, 20 and 26 lattices, showing the L dependence of the finite-size rounding effects near to the critical temperature.

$$B = 1.5 \pm 0.1.$$

Within error limits the critical exponent β coincides with the Ising value $\beta = 0.325$ [16].

The response of the spins to an applied small external magnetic field H defines the susceptibility χ. From equation (19) with $h = H/kT$ the relation to the spin fluctuations follows:

$$\chi = \frac{\partial m}{\partial H} = \frac{1}{kT}\frac{\partial^2}{\partial h^2}\ln Z$$

$$= \langle(\sigma - \langle\sigma\rangle)^2\rangle/kT = \Delta m^2/kT. \tag{33}$$

A log-log plot of $\ln \Delta m^2$ against $\ln|\varepsilon|$ is shown in figure 9. A linear fit within the 'critical windows' yields sufficiently accurate values for the exponents γ, γ' and amplitudes $C^{\pm}$ defined by

$$\Delta m^2 \approx \begin{cases} C^-|\varepsilon|^{-\gamma'} & T \uparrow T_c \\ C^+|\varepsilon|^{-\gamma} & T \downarrow T_c. \end{cases} \tag{34}$$

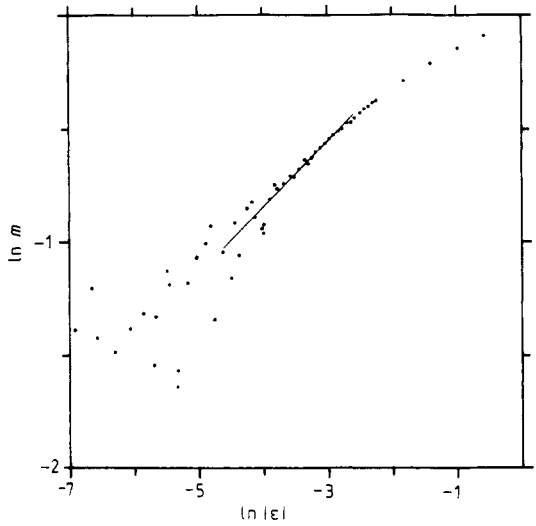

Figure 8. Log-log plot of the order parameter $\ln|m|$ against $\ln|\varepsilon|$ for a $L=26$ lattice. The linear fit in the 'critical window' yields the exponent and amplitude of (31) and (32).

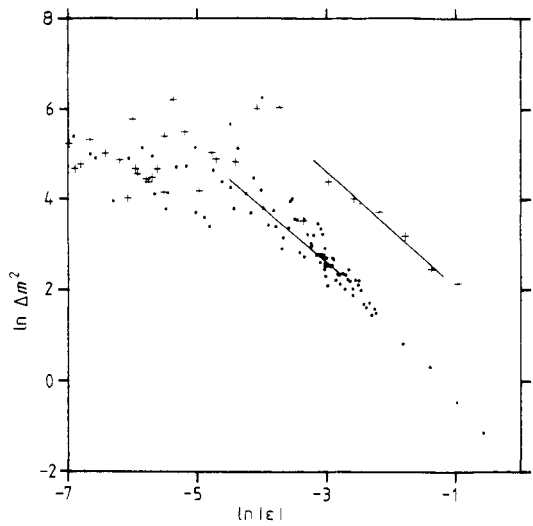

Figure 9. Log-log plot of the susceptibility $\ln \Delta m^2$ against $\ln|\varepsilon|$ for a $L=26$ lattice. The points and crosses correspond to the low and high temperature phases, respectively.

The Monte Carlo data imply

$$\gamma' = 1.22 \pm 0.05 \qquad C^- = 0.35 \pm 0.03$$
$$\gamma = 1.3 \pm 0.2 \qquad C^+ = 2.1 \pm 0.3. \tag{35}$$

Again, the critical exponents γ, γ' are compatible, within error limits, with the Ising value $\gamma = 1.24$ [16].

Next, the specific heat per site

$$c = \frac{\partial E}{\partial T} = \varepsilon_s \frac{\partial}{\partial T} \langle s \rangle / L^3 \tag{36}$$

is studied near the critical temperature T_c. From (2), it is related to the energy fluctuations

$$c/k\beta_s = \langle (s - \langle s \rangle)^2 \rangle / L^3 = \Delta s^2 / L^3. \tag{37}$$

The most singular part at $T \approx T_c$ defines the critical exponents α', α and amplitudes $A^{\mp}$ below and above T_c

$$\Delta s^2 / L^3 \approx \begin{cases} A^- |\varepsilon|^{-\alpha'} & T \uparrow T_c \\ A^+ |\varepsilon|^{-\alpha} & T \downarrow T_c. \end{cases} \tag{38}$$

A log-log plot of Monte Carlo data is shown in figure 10. The quantity $\ln(\Delta s^2/L^3)$ is plotted against $\ln|\varepsilon|$ for a 26^3 lattice. Unfortunately, for the specific heat the corrections to scaling seem to be more significant than for the other quantities discussed above. Hence the 'critical windows' for lattice sizes with reasonable computer time appear rather narrow. Therefore we obtain only very rough estimates for the critical exponents α' and α. The linear fits in figure 10 imply the exponents

$$\begin{aligned} \alpha' &= 0.2 \pm 0.1 \\ \alpha &= 0.3 \bullet 0.2 \end{aligned} \tag{39}$$

which are not in contradiction with the Ising value $\alpha = 0.11$ [16].

Using the definition of the magnetic field in equation (19) the scaling behaviour of the critical isotherm $m(h, T = T_c)$ for small values of $|h|$ is

$$m \approx D|h|^{1/\delta}. \tag{40}$$

To determine the critical exponent δ and the amplitude D in figure 11 $\ln(m)$ is plotted against $\ln|h|$ at the critical temperature $T = T_c$. The analysis of a linear fit in the 'critical window' gives

$$\begin{aligned} \delta &= 5.2 \pm 0.2 \\ D &= 1.37 \pm 0.05 \end{aligned} \tag{41}$$

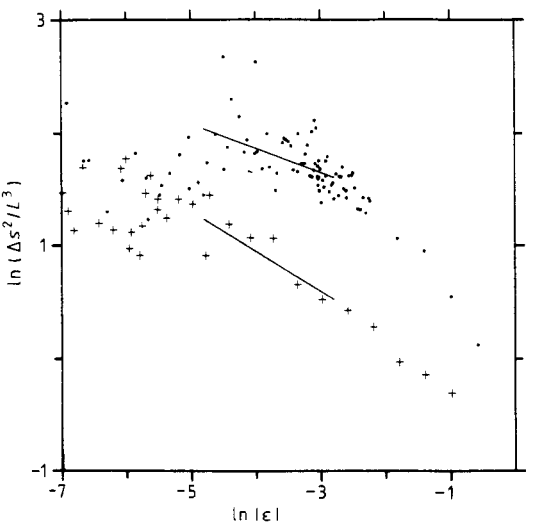

Figure 10. Log-log plot of the specific heat $\ln(\Delta s^2/L^3)$ against $\ln|\varepsilon|$ for a $L = 26$ lattice. Obviously, there is no reasonable linear behaviour range and the fits give only very rough estimates for the exponents α' and α.

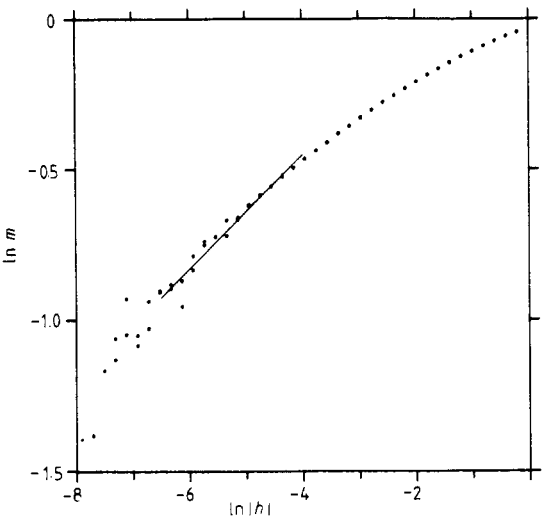

Figure 11. Log-log plot of the critical isotherm $m(h, T = T_c)$, $\ln|m|$ against $\ln|h|$ for a $L = 26$ lattice.

consistent (after finite-size extrapolation $L \to \infty$) with the Ising value $\delta = (2+d-\eta)/(2-d+\eta) = 4.9$ [16].

5. Critical behaviour of the intersection surface gas model

An analysis of the critical behaviour of the general intersecting surface gas model (along the critical lines for finite values of β_l) as detailed, has not been performed for the self-avoiding case (described in the previous section). But some Monte Carlo simulations for $\beta = 0.5$, 0 (the Ising case) and -0.4 support the conjecture that the model has Ising-like critical behaviour along the critical line from $\beta_l = \infty$ down to the tricritical point β_l^t.

At a tricritical point in three dimensions mean-field behaviour (up to logarithmic corrections) is expected [17]. This is in agreement with the Monte Carlo results to be presented in this section. For the determination of the tricritical exponents at the tricritical point (26) the intersection surface gas model was simulated on a lattice with size $L = 20$ and $T \leq T_t$. Figure 12 shows a log-log plot of the data for the order parameter m. A linear fit in the 'critical window' yields effective values for the exponent β_t and the amplitude B_t defined analogously to (29)

$$\begin{aligned} \beta_t^{\text{eff}} &= 0.21 \pm 0.02 \\ B_t^{\text{eff}} &= 1.8 \pm 0.3. \end{aligned} \tag{42}$$

Respecting finite-size corrections (which are obviously more significant for β compared with the other exponents, cf (32), (33) and (36), (42)) compatibility with the mean-field value for the tricritical exponent $\beta_t = \frac{1}{4}$ is found.

The singular behaviour for $T \approx T_c$ of the susceptibility can be read off figure 13 which shows a log-log plot of Δm^2. The linear fit implies the tricritical exponent γ_t'

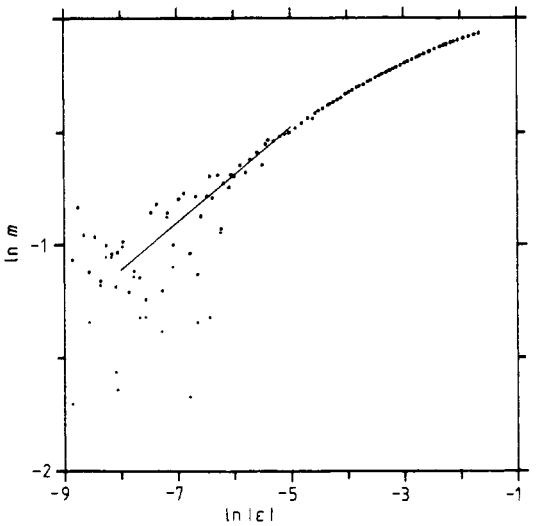

Figure 12. Log-log plot of the order parameter for the intersecting surface gas model at the tricritical point $\ln|m|$ against $\ln|\varepsilon|$ ($\varepsilon = (T - T_t)/T$) for a $L = 20$ lattice.

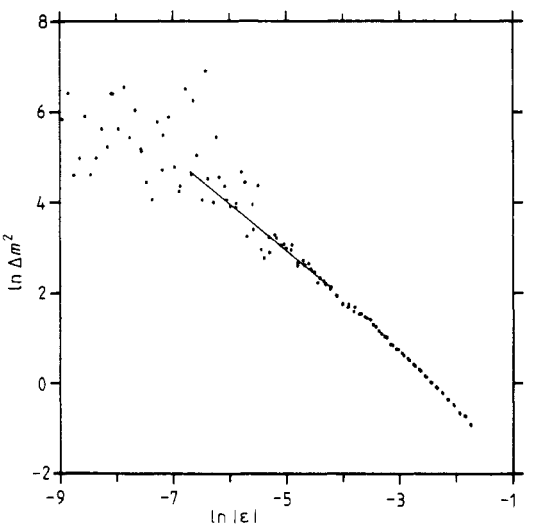

Figure 13. Log-log plot of the susceptibility at the tricritical point $\ln(\Delta m^2)$ against $\ln|\varepsilon|$ ($T < T_t$) for a $L = 20$ lattice.

and amplitude C_t^-:

$$\gamma_t' = 1.01 \pm 0.05$$
$$C_t^- = 0.11 \pm 0.02. \tag{43}$$

Correspondingly the log-log plot of the specific heat in figure 14 gives

$$\alpha_t' = 0.54 \pm 0.05$$
$$A_t^- = 0.42 \pm 0.05 \tag{44}$$

to be compared with the mean-field value $\alpha_t = \frac{1}{2}$.

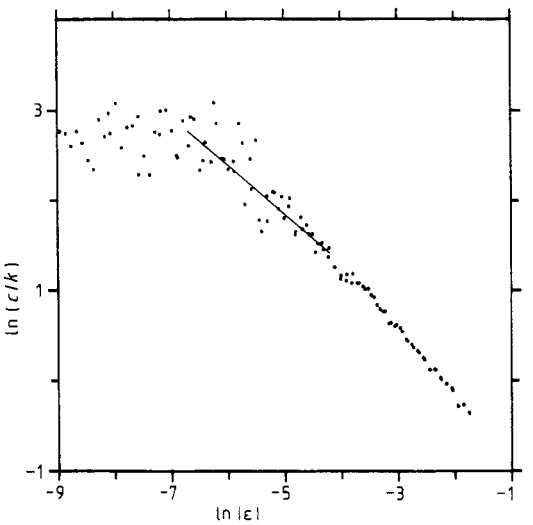

Figure 14. Log-log plot of the specific heat at the tricritical point $\ln(c/k)$ against $\ln|\varepsilon|$ ($T < T_t$).

The log-log plot in figure 15 of the tricritical isotherm of the order parameter at the tricritical point yields the exponent δ_t and amplitude D_t:

$$\begin{aligned} \delta_t &= 5.4 \pm 0.2 \\ D_t &= 1.6 \pm 0.4 \end{aligned} \tag{45}$$

whereas the mean-field value is $\delta_t = 5$.

Hence one can conclude that, taking finite-size extrapolations to $L = \infty$ into account, the Monte Carlo data for the intersecting random surface gas model at the tricritical

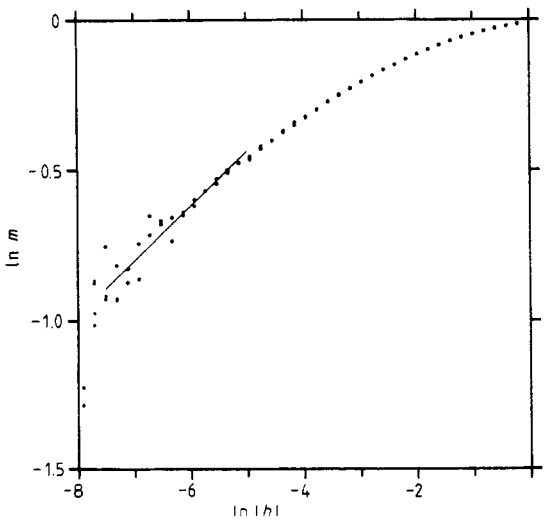

Figure 15. Log-log plot of the tricritical isotherm $m(h, T = T_t)$, $\ln|m|$ against $\ln|h|$ for a $L = 20$ lattice.

points given by (26) are consistent with mean-field behaviour which is expected in three dimensions [17].

6. The Hausdorff dimension of a self-avoiding planar random surface

In this section a model of a self-avoiding random surface with the fixed topology of the sphere is considered. The model is defined by the partition function (1) where the sum runs over all configurations of self-avoiding planar closed and connected surfaces on a cubic lattice. On the infinite lattice for low temperatures the surface has finite size and energy. Both diverge at the critical temperature T_c ($\beta_s^c = 0.53$, cf [9]). The average radius of gyration ξ (which is of the order of the correlation length) behaves for $T \uparrow T_c$ like

$$\xi \sim (T_c - T)^{-\nu}. \tag{46}$$

The critical exponent ν is related to the 'Hausdorff dimension' [18] of the surface

$$d_H = 1/\nu \tag{47}$$

which is defined (for $T \uparrow T_c$) by

$$d_H = \lim_{R\to\infty} \lim_{S\to\infty} \langle \ln s(R)\rangle(s)/\ln R. \tag{48}$$

The average $\langle\ \rangle(s)$ is taken only over configurations with energy s. The energy $s(R)$ is the number of plaquettes of the surface contained in a sphere (or for practical reasons a cube) with diameter R such that the surface passes its centre. It follows that, on average,

$$\langle s(R)\rangle \sim R^{d_H} \qquad \text{as } R\to\infty \tag{49}$$

for infinitely extended surfaces.

For a numerical determination of the 'Hausdorff dimension' by means of Monte Carlo simulations we proceed as follows. On a periodic lattice of size $L = 52$ for growing temperatures slightly below the critical one ($\beta = 0.54, \ldots, 0.53$ in steps of 0.0002) the average $\langle \ln s(R)\rangle(s)$ is determined as a function of the configurational energy s and the cube diameter R. The cubes are taken with diameter $R = 2, 3, \ldots, 10$ and the energies s in the intervals]1000, 1100], ...,]4900, 5000]. If the surface reaches a size such that it would touch itself around one period, the Monte Carlo run is restarted with $\beta_s = 0.54$ and a small surface. Five such restarts have been taken into account. After an extrapolation to $s\to\infty$ in the form

$$\langle \ln s(R)\rangle(s) = \langle \ln s(R)\rangle_\infty + O(1/s) \tag{50}$$

we obtain the function $\delta_H(R) = \langle \ln s(R)\rangle_\infty / \ln R$ which is plotted against $1/\ln R$ in figure 16. A linear extrapolation to $R\to\infty$ gives the Hausdorff dimension of a closed self-avoiding planar surface

$$d_H = 2.30 \pm 0.05. \tag{51}$$

This value is in good agreement with a Flory-type formula $d_H = (4+d)/3 = 2\frac{1}{3}$ derived in reference [19] and in less good agreement with a renormalisation group result $d_H = 2.5$ of the same authors.

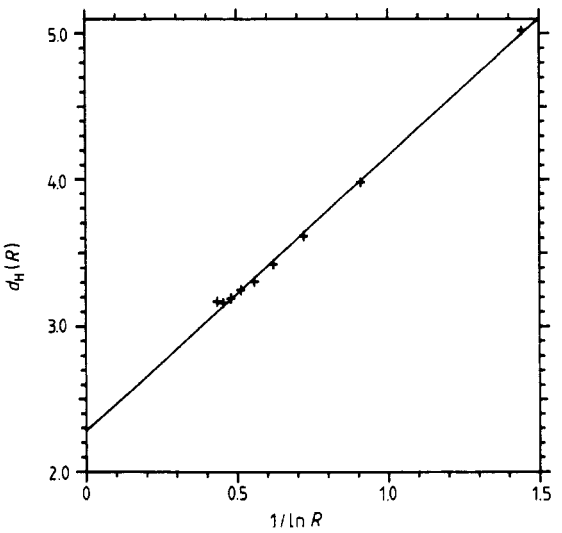

Figure 16. Plot of the function $\langle \ln s(R)\rangle_\infty/\ln(R)$ against $1/\ln(R)$ for a self-avoiding planar random surface. The area of the surface inside a cube with diameter R is $s(R)$ and $\langle\ \rangle_\infty$ means the extrapolation to an infinite surface. The value at $R=\infty$ gives the Hausdorff dimension $d_H = 2.3$.

7. Conclusions

The phase diagram of an intersecting random surface gas model has been analysed by means of Monte Carlo simulations. Lines of second- and first-order phase transitions, tricritical points and a point where the disordered phase coexists with four ordered ones have been found. As a main result Ising-like critical behaviour for the self-avoiding case, as well as along the critical lines, has been established. The Monte Carlo data

Table 1. Summary of Monte Carlo results for the self-avoiding surface gas model compared to the Ising values [16]. The exponents and amplitudes have been calculated at the critical point $\beta_c = 0.353$ on 26^3 lattices. For β and B in addition the finite-size extrapolated values are given.

Critical exponents and amplitudes	Self-avoiding surface model	Ising model [16]
β_{26}	0.29 ± 0.01	
B_{26}	1.4 ± 0.1	
β	0.32 ± 0.01	0.325
B	1.5 ± 0.1	
γ' $(T < T_c)$	1.22 ± 0.05	1.24
C^-	0.35 ± 0.03	
γ $(T > T_c)$	1.3 ± 0.2	1.24
C^+	2.1 ± 0.3	
α' $(T < T_c)$	0.2 ± 0.1	0.11
α $(T > T_c)$	0.3 ± 0.2	0.11
δ	5.2 ± 0.2	4.9
D	1.37 ± 0.05	

Table 2. Summary of Monte Carlo results for the intersecting surface gas model, compared to mean-field values. The exponents and amplitudes have been determined at the tricritical point $(\beta_s, \beta_l)^t = (0.568, -0.510)$ on 20^3 lattices.

Tricritical exponents and amplitudes	Intersecting surface model	Mean field
β_t	0.21 ± 0.02	0.25
B_t	1.8 ± 0.0	
γ_t'	1.04 ± 0.05	1
C_t	0.11 ± 0.02	
α_t'	0.54 ± 0.05	0.5
δ_t	5.4 ± 0.2	5
D_t	1.6 ± 0.4	

at the tricritical point are consistent with mean-field behaviour. The numerical results are summarised in tables 1 and 2. The Hausdorff dimension of a self-avoiding planar random surface has been calculated. The result $d_H = 2.30 \bullet 0.05$ is in agreement with a Flory-type formula [19]. There also exist preliminary Monte Carlo data [20] for the critical behaviour of the model of self-avoiding surfaces including Gaussian curvature energy which we considered in reference [1]. The data suggest that the critical behaviour is independent of the curvature energy and is Ising-like along the critical line discussed in reference [1]. However, it is expected that this model (and analogously models with 'bending' energy) also show non-universal critical behaviour in other regions of the parameter space. This shall be investigated in the future.

Acknowledgments

I gratefully acknowledge useful discussions with W Helfrich, F Rys, R Schrader, B Schroer and H J Thun. This work was supported by the Deutsche Forschungsgemeinschaft under contract no Schr. 4/10-1. The calculations were performed on the VAX 11/780 of the Fachbereich Physik der Freien Universität Berlin and on the Cray 1M of the Berlin Konrad-Zuse Rechenzentrum.

References

[1] Karowski M and Thun H J 1985 *Phys. Rev. Lett.* **54** 2556
[2] Symanzik K 1969 *Local Quantum Theory, Proc. Int. School of Physics 'Enrico Fermi', Course XLV* ed R Jost (New York: Academic) p 152
[3] Fröhlich J 1984 *Progress in Gauge Field Theory* ed G 't Hooft *et al* (*NATO Advanced Study Institute Series B* No 115) (New York: Plenum)
Schrader R 1985 *Commun. Math. Phys.* **102** 31
[4] Polyakov A 1981 *Phys. Lett.* **103B** 207
[5] Hofsäss T and Kleinert H 1984 *Phys. Lett.* **102A** 420
[6] de Gennes P and Taupin C 1982 *J. Phys. Chem.* **86** 2294
[7] Flory P J 1969 *Principles of Polymer Chemistry* (Ithaca, NY: Cornell University Press)
[8] Weeks J D 1979 *Ordering in Strongly Fluctuation Condensed Matter Systems* ed T Riste (New York: Plenum)
[9] Sterling T and Greensite J 1983 *Phys. Lett.* **121B** 345

[10] Eguchi T and Fukugita M 1982 *Phys. Lett.* **117B** 223
Kawai H and Okamoto Y 1983 *Phys. Lett.* **130B** 415
Berg B and Billoire A 1984 *Phys. Lett.* **298B** 297
Berg B, Billoire A and Foerster D 1985 *Nucl. Phys.* B **251** 665
Schrader R 1985 *J. Stat. Phys.* **40** 533
[11] Karowski M, Thun H J, Helfrich W and Rys F S 1983 *J. Phys. A: Math. Gen.* **16** 4073
[12] Karowski M and Rys F 1986 *J. Phys. A: Math. Gen.* **19** 2599
[13] Barber M N and Rys F S 1985 *Z. Phys.* B **58** 149
[14] Baxter R J 1982 *Exactly Solved Models in Statistical Mechanics* (New York: Academic)
[15] Wu F Y 1982 *Rev. Mod. Phys.* **54** 235
[16] Le Guillou J C and Zinn-Justin J 1980 *Phys. Rev.* B **21** 3976
[17] Wegner F J and Riedel E K 1975 *Phys. Rev.* B **7** 248
[18] Durhus B, Fröhlich J and Jonsson T 1984 *Phys. Lett.* **137B** 93
[19] Maritan A and Stella A 1984 *Phys. Rev. Lett.* **53** 123
[20] Karowski M and Thun H J 1986 *Monte Carlo Simulations for Self-Avoiding Surfaces* to be published
[21] Balian R, Drouffe J M and Itzykson C 1975 *Phys. Rev.* D **11** 2098